DMD Fast Forward. Published on June 9, 2017 as DOI: 10.1124/dmd.117.076489
This article has not been copyedited and formatted. The final version may differ from this version.

Oxetane Substrates of Human Microsomal Epoxide Hydrolase

Francesca Toselli, Marlene Fredenwall, Peder Svensson, Xue-Qing Li, Anders ~~M.~~ Johansson, Lars Weidolf and Martin A. Hayes

Cardiovascular and Metabolic Diseases, Innovative Medicines and Early Development, AstraZeneca, Pepparedsleden 1, Mölndal, 431 83, Sweden (F.T., M.F., X.-Q.L., A.~~M.~~J., L.W. and M.A.H.)

Integrative Research Laboratories, Arvid Wallgrens Backe 20, Gothenburg, 413 46, Sweden (P.S.)

DMD Fast Forward. Published on June 9, 2017 as DOI: 10.1124/dmd.117.076489
This article has not been copyedited and formatted. The final version may differ from this version.

Running title: Oxetane Substrates of Human Microsomal Epoxide Hydrolase

Address correspondence to:

Dr Martin A. Hayes,

Cardiovascular and Metabolic Diseases, Innovative Medicines and Early Development,

AstraZeneca,

Pepparedsleden 1, Mölndal,

431 83, Sweden.

Telephone: +46 (0) 31 776 2004

Fax: +46 (0) 31 776 3867

Email: martin.hayes@astrazeneca.com

Number of text pages: ~~29~~35

Number of tables: ~~2~~3

Number of figures: 3

Number of references: ~~28~~34

Number of words in *Abstract*: ~~249~~248

Number of words in *Introduction*: ~~377~~376

Number of words in *Discussion*: ~~1024~~1352

Non-standard abbreviations used are:

mEH, microsomal epoxide hydrolase; HLM, human liver microsomes; HLC, human liver cytosol; KTZ, ketoconazole; 1-ABT, 1-aminobenzotriazole; PRG, progabide; *t*-AUCB, *trans*-4-[4-(1-adamantylcarbamoylamino)cyclohexyloxy]benzoic acid; VPD, valpromide; *c*SO, *cis*-stilbene oxide; BSA, bovine serum albumin; 11,12-EET, (±)11,12-Eepoxy-5Z,8Z,14Z-eicosatrienoic acid; sEH, soluble epoxide hydrolase; P450, cytochrome P450, heme-thiolate protein P450; UHPLC-QTOF-MS, ultra-high performance liquid chromatography/quadrupole time-of-flight mass spectrometry; CE, collision energy.

Abstract

Oxetanyl building blocks are increasingly used in drug discovery because of the improved drug-like properties they confer on drug candidates, yet little is currently known about their biotransformation. A series of oxetane-containing analogues was studied and we provide the first direct evidence of oxetane hydrolysis by human recombinant microsomal epoxide hydrolase (mEH). Incubations with human liver fractions and hepatocytes were performed with and without inhibitors of P450s, mEH and soluble EH (sEH). Reaction dependence on NADPH was investigated in subcellular fractions. A full kinetic characterization of oxetane hydrolysis is presented, in both human liver microsomes and human recombinant mEH.

In human liver fractions and hepatocytes, hydrolysis by mEH was the only oxetane ring-opening metabolic route, with no contribution from ~~cytosolic~~ sEH or from cytochromes P450-catalyzed oxidation. Minimally altering the structural elements in the immediate vicinity of the oxetane can greatly modulate the efficiency of hydrolytic ring cleavage. In particular, higher pK_a in the vicinity of the oxetane and an increased distance between the oxetane ring and the benzylic nitrogen improve reaction rate, which is further enhanced by the presence of methyl groups near or on the oxetane. This work defines oxetanes as the first non-epoxide class of substrates for human mEH, which was previously known to catalyze the hydrolytic ring-opening of electrophilic and potentially toxic epoxide-containing drugs, drug metabolites and exogenous organochemicals. These findings will be of value for the development of biologically active oxetanes and may be exploited for the biocatalytic generation of enantiomerically pure oxetanes and diols.

Introduction

Oxetane rings are becoming widely incorporated in novel drug design because of the improved properties which they confer on drug candidates (Wuitschik et al., 2010; Bull et al., 2016). The use of oxetanyl groups as alternatives to e.g. gem-dimethyl groups leads to a significant increase in solubility and lower lipophilicity whilst maintaining steric bulk (Wuitschik et al., 2010; Bull et al., 2016). The introduction of the spiro-oxetanylazetidinyl moiety has also been pursued as a means of providing favorable physico-chemical and pharmacokinetic properties compared to larger ring systems (Wuitschik et al., 2010; Bull et al., 2016) and was recently reported in the discovery of the melanin-concentrating hormone receptor antagonist AZD1979 (Supplemental Figure 1) (Johansson et al., 2016). In subsequent studies using selective inhibitors in human liver fractions, hydrolytic ring-opening of the spiro-oxetanyl ring system in AZD1979 was observed and found to be a novel reaction catalyzed by the human microsomal epoxide hydrolase (mEH) (Li et al., 2016).

mEH (EC 3.3.2.9) is a highly conserved drug-metabolizing enzyme and a member of the α/β-hydrolase fold family of proteins (Morisseau and Hammock, 2005; Vaclavikova et al., 2015). mEH is widely expressed in the human body and typically catalyzes the hydrolytic ring-opening of epoxide-containing exogenous organochemicals, thus playing an important role in the detoxification of ~~e.g.~~ electrophilic and potentially toxic drugs and drug metabolites (Morisseau and Hammock, 2005; Vaclavikova et al., 2015).

For the continued development of oxetane-containing drug candidates, knowledge on the enzymology of their metabolism is crucial in order to predict drug-drug interaction risk, to model drug exposure in a variety of patient populations and to fulfil regulatory requirements. The objective of the present study was to investigate simple oxetanyl analogues of AZD1979 and to

DMD Fast Forward. Published on June 9, 2017 as DOI: 10.1124/dmd.117.076489
This article has not been copyedited and formatted. The final version may differ from this version.

probe the influence on metabolic ring-opening of different structural features in the vicinity of the oxetanyl ring. It is shown that oxetanes are exclusively ring-opened *via* hydrolysis by human mEH and that several structural variations in the vicinity of the oxetane greatly affect the ~~extent~~ rate of hydrolysis. Oxetane hydrolysis by human recombinant mEH, with full kinetic parameters, is also reported, providing the first direct evidence of this new activity of human mEH. This work describes a new class of substrates for this important enzyme and defines hydrolysis as a major metabolic ring-opening pathway for oxetanes.

Materials and Methods

Materials

Pooled, mixed-gender human liver microsomes (HLM) were purchased from BD Biosciences (Bedford, MA, USA). Pooled, mixed-gender human liver cytosol (HLC) and cryopreserved hepatocytes were purchased from Bioreclamation IVT (Frankfurt am Main, Germany). Recombinant human mEH was a generous gift from Prof. B. D. Hammock (University of California Davis, Davis, CA, USA). Ketoconazole (KTZ), 1-aminobenzotriazole (1-ABT), progabide (PRG) and *trans*-4-[4-(1-adamantylcarbamoylamino)cyclohexyloxy]benzoic acid (*t*-AUCB) were obtained from AstraZeneca Compound Management (AstraZeneca R&D Gothenburg, Sweden). Valpromide (VPD), styrene oxide (SO), *cis*-stilbene oxide (*c*SO), hydrobenzoin (the product of *c*SO ring-opening), bovine serum albumin (BSA, catalogue number A9418) and NADPH were purchased from Sigma Aldrich (St. Louis, MO, USA). (±)11,12-~~epoxy~~Epoxy-5Z,8Z,14Z-eicosatrienoic acid (11,12-EET) was purchased from Cayman Chemicals (Ann Arbor, MI, USA). Oxetanes **1-9**, **15-20** and diols **10-14**, **21** and **22** were synthesized and characterized at Medicinal Chemistry, Cardiovascular and Metabolic Diseases, Innovative Medicines and Early Development Biotech Unit, AstraZeneca (Gothenburg, Sweden), as detailed in the supplemental methods. All other chemicals were of the highest quality commercially available.

Incubations with human liver subcellular fractions and selective inhibitors

The contribution of different liver enzymes to the metabolism of compounds **1-9** and **15-20** (see Tables 1 and 2 for structures) was monitored in HLM and HLC in the presence of inhibitors. *c*SO and 11,12-EET were used in parallel incubations as positive controls for metabolism by mEH and soluble EH (sEH), respectively (Chacos et al., 1983; Gill et al., 1983a). The following inhibitors

DMD Fast Forward. Published on June 9, 2017 as DOI: 10.1124/dmd.117.076489
This article has not been copyedited and formatted. The final version may differ from this version.

were used (final concentrations): KTZ (P450 inhibitor; 200 µM), VPD (mEH inhibitor; 10-1000 µM) or PRG (mEH inhibitor; 100 µM), in HLM; and VPD (200 µM) or *t*-AUCB (sEH inhibitor; 20 µM), in HLC. Concentrations of all inhibitors were chosen to be in excess of their inhibition constants reported in the literature (Kerr et al., 1989; Kroetz et al., 1993; Emoto et al., 2003; Liu et al., 2009); at the concentration used, KTZ was expected to inhibit all major liver cytochromes P450 (P450) (Emoto et al., 2003).

Compounds **1-9** (10 µM) or *c*SO (100 µM) were incubated individually with either HLM or HLC (1 mg protein/ml) in sodium phosphate buffer (0.1 M, pH 7.4, 50 µl) for 1 hour at 37 °C with constant shaking. Compounds **15-20** were incubated in the same manner, but only with HLM, whereas 11,12-EET (10 µM) was incubated ~~in the same manner, but~~ only with HLC. The subcellular fractions were pre-incubated in buffer with or without NADPH (1 mM) plus inhibitor or vehicle for 3 minutes, then reactions were started by the addition of substrate. Chemical stability of compounds **1-9** and **15-20** in buffer was also assessed in similar incubations, lacking the liver fractions and the inhibitors. Final solvent concentrations were kept constant in all reactions and were ≤ 0.3 % (v/v) acetonitrile and ≤ 1.1% (v/v) DMSO; incubations with PRG and matching controls also contained 0.5% (v/v) methanol; incubations in HLC with 11,12-EET also contained 1.6% (v/v) ethanol. All assays were performed in duplicate, in round-bottom 96-well plates.

Reactions were quenched by mixing with either one (*c*SO) or three (**1-9**, **15-20** and 11,12-EET) volumes of ice-cold acetonitrile. After centrifugation at 4,000x*g* for 20 min, 50 µL of the supernatant were mixed with an equal volume of water, and the resulting mixture was analyzed by either ultra-high performance liquid chromatography/quadrupole time-of-flight mass spectrometry (UHPLC-QTOF-MS; **1-9**, **15-20** and 11,12-EET) or UHPLC/UV (*c*SO), as described in detail below.

DMD Fast Forward. Published on June 9, 2017 as DOI: 10.1124/dmd.117.076489
This article has not been copyedited and formatted. The final version may differ from this version.

Incubations with human hepatocytes

The metabolism of **1-9**, **15-20** and *c*SO was also assessed in human hepatocytes, with or without inhibitors. Inhibitors used were (final concentrations): 1-ABT (P450 inhibitor; 1-2 mM), VPD (100-200 µM) or *t*-AUCB (10-20 µM). At the concentrations used, 1-ABT was expected to ~~strongly~~ inhibit strongly all major liver P450s (Emoto et al., 2003).

Cryopreserved hepatocytes were thawed and resuspended in Leibovitz's L-15 medium to a final concentration of 10^6 cells/ml. Cells were pre-incubated for 7 minutes at 37 °C with inhibitor or vehicle under constant shaking, and reactions were then initiated by the addition of substrate (4 µM). Chemical stability of substrates in Leibovitz's L-15 medium was assessed in similar incubations, lacking hepatocytes and inhibitors. Final solvent concentrations were 0.04% DMSO and 0.08% acetonitrile in all reactions, and incubations (50 µL) were performed in duplicate, in flat-bottom 96-well plates. Reactions were quenched after 2 hours and processed as described above for incubations with subcellular fractions.

Determination of kinetic constants for oxetane hydrolysis

Human recombinant mEH and HLM were used to examine the kinetics of oxetane hydrolysis. Conditions for linear product formation with respect to time and protein concentration were assessed with the lowest substrate concentration later used in the substrate-saturation curves. No or negligible hydrolysis of oxetanes in compounds **1-3**, **8** and **9** was observed in these preliminary assays, thus further kinetic experiments were only performed with compounds **4-7**. From the second set of compounds **15** and **18** were selected for full kinetic characterization.

In assays with the recombinant enzyme, substrates (5-200 µM for compounds **5-7**, ~~or~~ 5-300 µM for compound **4**, or 10-200 µM for compounds **15** and **18**) were incubated with 1.9 µg/ml

DMD Fast Forward. Published on June 9, 2017 as DOI: 10.1124/dmd.117.076489
This article has not been copyedited and formatted. The final version may differ from this version.

(compounds **4**-**7**) or 5.6 µg/ml (compounds **15** and **18**) of recombinant mEH, for either 10 min (compound **6**), 30 min (compounds **5** and **7**), ~~or~~ 40 minutes (compound **4**) or 60 minutes (compounds **15** and **18**). The recombinant enzyme was thawed and diluted in cold Tris-HCl buffer (0.1 M, pH 9.0) supplemented with 0.1 mg/ml BSA, which is necessary to stabilize the purified protein and help solubilize lipophilic substrates (Morisseau and Hammock, 2007). This mixture was pre-incubated at 37 °C with constant shaking for 5 minutes, before starting the reactions with the addition of substrate (100 µl final reaction volume). An identical volume of substrate solution was added to each reaction directly from high-concentration acetonitrile stocks (compounds **4**-**7**) or acetonitrile/DMSO stocks (compounds **15** and **18**), to maintain the final solvent concentration ~~at 2~~≤ 3% (v/v) in all incubations. mEH activity has been reported to be unaffected by acetonitrile or DMSO concentrations up to 3% (v/v) (Seidegard and DePierre, 1980; Muller et al., 1997). Reactions were quenched and processed as described above. All assays were performed in duplicate (compound **4**, **15** and **18**) or triplicate (all other substrates), in round-bottom 96-well plates. To build calibration curves, synthetic diol standards **10**-**13**, **21** and **22** (0.01~~75~~-2.5 µM) were incubated, processed and analyzed in the same manner as the substrates, except without enzyme.

Kinetic experiments with HLM were performed similarly, but with the following exceptions: substrates (10-200 µM for compounds **5**-**7**, **15** and **18** or 10-300 µM for compound **4**) were incubated with 5 µg/ml (compounds **4**-**7**) or 15 µg/ml (compounds **15** and **18**) of HLM protein for 40 min (compounds **4**-**7**) or 60 min (compounds **15** and **18**), in sodium phosphate buffer (0.1 M, pH 7.4). Assays were performed in duplicate (compound **7**, **15** and **18**) or triplicate (all other substrates) and the concentration range for calibration curves with synthetic diol standards was 0.1~~25~~-5 µM.

DMD Fast Forward. Published on June 9, 2017 as DOI: 10.1124/dmd.117.076489
This article has not been copyedited and formatted. The final version may differ from this version.

Under the conditions used, with no other metabolite formed than the ring-opened diol, substrate depletion did not exceed 6% with either enzyme system.

*Determination of IC_{50} for inhibition of cSO hydrolysis by VPD and compounds **1-9***

Human recombinant mEH was diluted to 1.9 µg/ml in Tris-HCl buffer (0.1 M, pH 9.0) containing 0.1 mg/ml BSA. Compounds **1-9** (0-200 µM) or valpromide (0-2 mM) were added from acetonitrile stocks and the mixture was pre-incubated for 5 min at 37 °C with constant shaking. Then *c*SO was added from a DMSO stock to a final concentration equal to its K_m (140 µM with the human recombinant enzyme (Morisseau et al., 2011)) and incubated for a further 10 min. Preliminary experiments confirmed a linear hydrobenzoin product formation in these conditions (data not shown). Final solvent concentrations were 0.56% DMSO and 2% acetonitrile in all incubations (100 µl total reaction volume). All assays were performed in triplicate in round-bottom 96-well plates. Generation of calibration curves and processing of the reactions were done as described in the previous section.

Metabolite profiling and data analysis for selective inhibition assays

For incubations with **1-9**, **15-20** or 11,12-EET, UHPLC-QTOF analysis of metabolites from selective inhibition assays was performed as described previously (Li et al., 2016), with the following modifications: a different gradient profile was used with the initial mobile phase (90:10 A:B) transitioning to 70:30 A:B over 6 minutes and the mass spectrometer was a Synapt G2 Q-TOF (Waters). Mobile phase A was 0.1% formic acid in water (for reactions with oxetanes or 11,12-EET) or water (for reactions with *c*SO) and mobile phase B was acetonitrile. An MS^E method with two separate scan functions programmed with independent collision energies (CEs) was used for data acquisition. Trap CE in function 1 was 4 V and in function 2 an energy ramp of

15–35V was used; the transfer cell CE was 20 V. The entire system was operated using MassLynx (Waters, version 4.1), and data were processed with MetaboLynx V4.1. MS and MS^E spectra were compared between the parent compound and metabolites to identify metabolite structures and site(s) of modification in the substrate molecule. UHPLC/Q-TOF MS^E characteristics of compounds **1-9** and their hydrated metabolites are listed in Supplemental Table 1, although no MS^E spectra could be obtained for compounds **15-20**. Products from reactions with *c*SO were analyzed by UV detection. The UHPLC eluate was introduced into an Acquity UV-PDA detector (Waters), and the diol hydrobenzoin metabolite in the experimental samples was identified by comparing the retention time with that of the authentic standard. Retention times for hydrobenzoin and *c*SO were 3.27 and 5.38 min, respectively. Metabolite peaks on the trace from the full UV scan (210-400 nm) were integrated using the TargetLynx™ tool (Waters). Peak areas were used for the relative quantification of diol metabolites in HLM incubations without NADPH (reported in Table 1), by calculating:

$$Relative\ diol\ \% = \frac{Diol_{area}}{Diol_{area} + Parent_{area}} \times 100$$

For incubations with inhibitors (or those lacking NADPH), relative diol levels were expressed as a percentage of the corresponding peak areas in control incubations with vehicle and NADPH.

Metabolite quantification and data analysis for kinetic assays

Chromatographic separation of metabolites from kinetic assays ~~with compounds **4-7**~~ was performed on an Acquity UHPLC HSS T3 column (2.1×100 mm, 1.8 µm; Waters; for compounds **4-7**) or an Acquity UHPLC BEH column (2.1x100 mm, 1.7 µm; Waters; for compounds **15** and **18**) operated by an Acquity UHPLC system. To improve the separation between diols and parent compounds, mobile phase A was changed from 0.1% aq. formic acid to

DMD Fast Forward. Published on June 9, 2017 as DOI: 10.1124/dmd.117.076489
This article has not been copyedited and formatted. The final version may differ from this version.

10 mM ammonium acetate in water; mobile phase B was acetonitrile. The initial mobile phase was 90:10 A:B, transitioning to 10:90 A:B over 6 minutes using a linear gradient, with a 7.7 min total run time. The flow rate was 0.5 ml/min and the column oven was set to 45 °C. A one-minute window of UHPLC eluate, centred on the retention time of each diol metabolite, was introduced into a Xevo® G2-S Q-TOF mass spectrometer (Waters; for compounds **4-7**) or a Synapt G2 Q-TOF (Waters; for compounds **15** and **18**), operating as described above. Diols formed in incubations with compounds **4-8**, **15** and **18** were quantified by external calibration as described in the previous sections, using TargetLynx™ (Waters). The extracted ion chromatograms corresponding to the protonated molecular ion of the diol were generated with a mass tolerance of 30 mDa.

To determine K_m and V_{max}, initial velocities were plotted versus the corresponding substrate concentration and fitted to the Michaelis-Menten equation by nonlinear regression, using GraphPad Prism version 6.07 for Windows (GraphPad Software, La Jolla, CA, USA).

Detection and quantification of hydrobenzoin formed in IC_{50} assays with *c*SO was performed by UHPLC/UV as described in the previous section, except that 10 mM ammonium acetate was used as mobile phase A instead of water, to avoid co-elution of hydrobenzoin with oxetanes or diols. Velocities of hydrobenzoin formation were plotted against the logarithm of the corresponding inhibitor concentration and fitted to the one-site competitive binding equation by nonlinear regression, using GraphPad Prism.

Calculations of ring-strain energies and determination of pK_a

A detailed account of ring-strain energy calculations for relevant truncated fragments of compounds **1-9** is given in the Supplemental material. Determination of solubility and logD for

DMD Fast Forward. Published on June 9, 2017 as DOI: 10.1124/dmd.117.076489
This article has not been copyedited and formatted. The final version may differ from this version.

all oxetanes, and pK_a values for compounds **1-9** was performed as described earlier (Boström et al., 2012).

DMD Fast Forward. Published on June 9, 2017 as DOI: 10.1124/dmd.117.076489
This article has not been copyedited and formatted. The final version may differ from this version.

Results

Oxetanes are opened exclusively via hydrolysis by mEH

Compounds **1-9**, **15-20**, *c*SO and 11,12-EET were incubated with human liver subcellular fractions or hepatocytes in the presence or absence of inhibitors of P450s, mEH and sEH. Ring-opening of the substrates in incubations with liver fractions was also monitored with or without NADPH.

All oxetanes were metabolized to a variety of products in the presence of NADPH (see Figure 1A for an example with compound **5** incubated with HLM). Metabolites included products with a mass increase of 18 Da (H_2O) with respect to substrate and its *N*- or *O*-demethylation products. The oxetanylmethylaminyl moiety was the only part of each compound not retained in any of the fragment ions detected under the MS^E conditions used, and no fragment of the hydrated metabolite showed a mass shift of +18 Da relative~~ly~~ to that of the parent (see representative MS and MS^E spectra for compound **5** in Figure 2 and MS and MS^E data for all compounds in Supplemental Table 1). The hydrated metabolites formed from each parent compound were then found to co-elute with the corresponding synthesized diols (see Figure 1B for representative chromatograms for compound **5** and Supplemental Figure 5 for the synthetic diol structures), and MS^E spectra of each metabolite/synthetic diol pair were identical (Figure 2).

Hydration (addition of the elements of H_2O) for all test compounds was NADPH-independent in incubations with HLM (see Figure 3 for an example with compound **6** and Supplemental Figure 2 for all other compounds). In contrast, the formation of diols from ~~compounds **1-9**~~all oxetanes and the mEH probe substrate *c*SO, but not from the sEH probe substrate 11,12-EET, was essentially abolished in the presence of high concentrations of the mEH inhibitor VPD in liver fractions and hepatocytes (Figure 3 and Supplemental Figure 2). Similar results were obtained with the structurally unrelated mEH inhibitor PRG (data not shown). High concentrations of the P450

inhibitors KTZ and 1-ABT did not inhibit hydration of any compound (Figure 3 and Supplemental Figure 2), while greatly decreasing demethylation of compounds **1**, **3**, **5-7**, ~~and~~ **9** and **15-20** (data not shown), indicating that a functional P450 system was present and could be effectively inhibited in the assay conditions used. Some degree of inhibition of diol formation by P450 inhibitors was observed for a compounds **4** and **15-17** in HLM and **2**, **5**, **8** and **16-17** in hepatocytes (Supplemental Figure 2), but this was also observed for hydrolysis of the mEH probe substrate *c*SO (Supplemental Figure 2). In addition, incubation of these and the other oxetanes with both NADPH and VPD completely abolished diol formation (Figure 3 and Supplemental Figure 2). These data suggested that the apparent reduction of oxetane hydrolysis by P450 inhibitors for these compounds was likely due to experimental variation between samples, rather than a true contribution of P450s to oxetane ring-opening. Conversely, diol formation from other compounds (**1-3**, **6-7** and **15-18** in HLM and **3**, **4**, **6**, **7** and **9** in hepatocytes) increased in the absence of a functional P450 system (i.e. either in incubations without NADPH or in the presence of KTZ or 1-ABT; Figure 3 and Supplemental Figure 2), while formation of the demethylated metabolites increased when mEH was inhibited (data not shown). Thus, inhibition of P450, or lack of NADPH, increased the availability of substrate for mEH-mediated metabolism, and conversely, inhibition of mEH increased substrate availability for P450 mediated metabolism. This indicated an apparent competition between mEH and P450s for the substrate and a lack of nonspecific inhibition of P450 activity by mEH inhibitors. Co-incubation with the sEH inhibitor *t*-AUCB ~~also~~ failed to inhibit hydration of ~~compounds **1-9**~~ oxetanes and *c*SO in hepatocytes (Figure 3 and Supplemental Figure 2), whereas it abolished hydrolysis of the sEH probe substrate 11,12-EET in HLC (Supplemental Figure 2). The same pattern of inhibition of oxetane hydration seen in HLM and hepatocytes by VPD ~~and *t*-AUCB~~ was also observed in HLC, where minor NADPH-independent diol formation occurred (Figure 3 and Supplemental Figure 2). This is

DMD Fast Forward. Published on June 9, 2017 as DOI: 10.1124/dmd.117.076489
This article has not been copyedited and formatted. The final version may differ from this version.

likely due to low levels of mEH contamination in the cytosol, as previously reported (Gill et al., 1982; Gill et al., 1983b). No diol formation was observed when the enzyme source was omitted (Figure 3 and Supplemental Figure 2). The inhibitory profile seen with the selective EH inhibitors VPD and *t*-AUCB against hydrolysis of the probe substrates *c*SO and 11,12-EET indicated that the assay was specific and effective at differentiating between metabolism catalyzed by the two forms of human EH.

Specific structural elements modulate oxetane hydrolysis in HLM and hepatocytes

The oxetane substrates were hydrolyzed to varying degrees by mEH (Tables 1 and 2). Diol formation was absent or minor for compounds **1-3**, ~~and~~ **9** and **15-20**, but was a major metabolic route for compounds **4-8**. Among the full-length analogues, poor (**1-3** and **9**) and good (**4-8**) oxetane substrates also had significantly different pK_a values (6.5±0.2 and 8.2±0.1, respectively; $p<0.001$, two-tailed unpaired T test; Table 1), though similar solubilities, lipophilicities (Table 1) and theoretical ring strain energies (Supplemental Table 2). This trend in pK_a was however not observed for the chain-shortened analogues (**15-20**), which showed broadly similar calculated pK_a values (Table 2).

Human recombinant mEH hydrolyses oxetanes with the same substrate preference as HLM

To more fully understand the interaction of mEH with oxetanes, ~~the~~ kinetic parameters for the hydrolysis of each of the full-length analogues (**1-9**) and two of the chain-shortened analogues (**15** and **18**) were determined in separate incubations with human recombinant mEH or HLM. Among the full-length compounds **1-9**, both enzyme systems showed the same substrate preference and only efficiently hydrolyzed compounds **4-7**. All four compounds **4-7** exhibited Michaelis-Menten type kinetics with both the recombinant enzyme and HLM and showed similar

K_m values (Table ~~2~~3; substrate-saturation curves are in Supplemental Figures 3 and 4). Hydrolysis of compounds **15** and **18** was less efficient and meant that K_m and V_{max} could only be determined with HLM, since within the substrate concentration range chosen, velocity remained linear with the recombinant enzyme (Table 3 and Supplemental Figures 3 and 4). No inhibition of *c*SO metabolism by compounds **1-9** was observed with recombinant mEH when using a substrate concentration corresponding to its K_m (data not shown). VPD, when tested under the same conditions, inhibited *c*SO hydrolysis with an IC_{50} of 7.1±0.3 µM.

Discussion

Oxetanes are being increasingly incorporated into the design of novel biologically active molecules (Wuitschik et al., 2010; Bull et al., 2016), yet there are few detailed reports on their biotransformation. Here we have shown that the oxetane moiety in a series of analogues can be~~is~~ consistently metabolized to a diol metabolite via hydrolysis by mEH, without contributions by any other enzyme system, and that this pathway may~~can~~ represent a major metabolic route depending on the structural context in which the oxetane is embedded. Oxetane rings thus represent a new class of substrates for human mEH.

An earlier study by Stepan and coworkers (2011) was the first to report metabolic ring cleavage of oxetanyl moieties in HLM (Stepan et al., 2011), but it was unclear which enzyme specifically catalyzed the formation of diol metabolites. A more recent study described an example of an oxetane-containing drug, EPZ015666, where the oxetanyl moiety was directly attached to a bicyclic aromatic core (Rioux et al., 2016). This compound was found to undergo ring-opening to diol via P450-mediated oxidation, likely via α-hydroxylation, ring-opening to the aldehyde and finally reduction to diol (Rioux et al., 2016). This is in contrast to our recent (Li et al., 2016) and

DMD Fast Forward. Published on June 9, 2017 as DOI: 10.1124/dmd.117.076489
This article has not been copyedited and formatted. The final version may differ from this version.

current findings and suggests that the environment of the oxetanyl moiety is key to determining the metabolic fate of this class of compounds.

In the series of analogues analyzed in this study, altering the structural elements in the vicinity of the oxetane greatly affected the efficiency of hydrolytic ring cleavage by mEH. Seven compounds were studied initially (**1-7**), of which four (**4-7**) showed more than 10% hydrolysis. While these data are semi-quantitative, not taking the potentially different MS response between the diols and corresponding parent into account, they served the purpose of dividing the compounds into two groups: poor (**1-3**) and good (**4-7**) mEH substrates. This grouping was later supported when the compounds were tested with recombinant mEH. Two structural elements were present only in the compounds (**4-7**) most prone to hydrolysis, but were lacking from the others: 3-methyl substitution on the oxetane ring and a methylene group between the oxetane ring and the benzylic nitrogen. Two additional analogues were then synthesized, each containing only one of these structural elements (compounds **8** and **9**). Addition of the 3-methyl substitution on the oxetane ring (compound **9**) led to traces of diol formation, whereas introduction of a methylene spacer between the oxetane and the basic N (compound **8**) led to an almost two-fold increase in diol formed from the similarly substituted oxetane **3**. This indicated that hydrolysis could be improved by the presence of a methylene spacer (compounds **8** vs **3**). Methyl substitutions alone, whether on oxetane (**9**) or benzylic nitrogen (**1**), do not affect hydrolysis, but in combination with the methylene spacer (**4-7**) each methyl substitution leads to a 5-fold increase in hydrolysis. To build on these initial structure-metabolism observations and to confirm that the specific enzymology of oxetane hydrolysis was retained with a minimal oxetane-containing substrate, a set of chain--shortened analogues was synthesized with masses ranging from 221 to 318 Da (**15-20**) (as outlined in the Supplemental Materials and Methods). Specifically the new set of compounds were analogues of compounds **4-8**, where the 4-

methoxyphenyl-oxadiazole amide--linked azetidine moiety had been replaced with a methyl group on the central phenyl ring. One analogue (**17**) was prepared in which the 4-methoxyphenyl-oxadiazole was replaced with an acetoxy substitution on the central azetidine.

While hydrolysis was less efficient than that of the full-length analogues, most likely due to the lower lipophilicities of compounds **15-20**, the chain-shortened analogues were still exclusively hydrolyzed by mEH, with no contributions from either P450s or sEH. A higher rate of hydrolysis of compounds **15-20** was observed with increasing methylation, as observed with the full-length analogues, whereas the presence of a methylene spacer between the amine and the phenyl ring decreased it.

When physico-chemical parameters were considered as potential predictors of hydrolysis rate, it was initially observed that among the full-length analogues **1-9**, good mEH substrates (**4-8**) had significantly higher pK_a's, but this did not apply to the set of chain-shortened compounds **15-20**, which had calculated pK_a values similar to those of compounds **4-8** despite being hydrolyzed at a considerably lower rate. Similarly, no trends in solubility, lipophilicity or calculated ring strain energy was observed between good and poor substrates, indicating that hydrolysis efficiencies are likely determined by ~~transition state and~~ active site binding properties ~~rather than differences in ring strain~~.

Importantly, the current work presents the first direct evidence of mEH-catalyzed oxetane hydrolysis with recombinant human mEH, which hydrolyzed oxetanes with the same substrate preference as human liver mEH. Kinetic experiments showed some variation in clearance (V_{max}/K_m) between substrates, and when compared to that of mEH probe substrates, oxetane clearance was lower than that for *c*SO, but similar to, or higher than that of styrene oxide (for reactions with HLM; (Seidegard and DePierre, 1980; Pacifici et al., 1986; Eugster et al., 1991)). Low K_m and reaction rates are common for EHs, with turnover numbers for mEH substrates

usually being lower than 1 s^{-1} (Oesch et al., 2000). This can be explained by the reported two-step catalytic mechanism for EHs: (1) The substrate rapidly binds to the active site forming a Michaelis complex, which then reversibly alkylates the enzyme forming an ester intermediate; (2) This intermediate then undergoes hydrolysis to form the corresponding diol ((Armstrong, 1999); for a schematic illustrating reaction of a spiro-oxetane substrate with mEH, see (Li et al., 2016)). The alkylation of the enzyme proceeds at a much faster rate (~three orders of magnitude faster) than the hydrolysis of the ester bond (Tzeng et al., 1996), resulting in an accumulation of the ester intermediate and a low rate of product formation (Oesch et al., 2000). Therefore, low K_m values have been suggested to reflect a high degree of enzyme alkylation, rather than a high affinity for the enzyme active site (Tzeng et al., 1996). ~~However l~~Low rates of product formation thus do not necessarily reflect a low efficiency of substrate consumption, as the enzyme may bind more substrate than it forms diol (Oesch et al., 2000). Additionally,~~:~~ where mEH is highly expressed, e.g. in human liver (Thomas et al., 1982; de Waziers et al., 1990; Song et al., 2015), its concentration may exceed that of the substrate and thus substrate depletion *in vivo* may be more efficient than what is suggested by *in vitro* kinetic profiles~~thus it may consume more substrate than it forms diol (Oesch et al., 2000)~~. Nonetheless, the kinetic parameters evaluated according to the Michaelis-Menten model provide a means to compare the test compounds and their propensity to undergo hydrolysis by mEH.

The name of the studied enzyme implies that only epoxides are accepted substrates and therefore our findings on the broader substrate specificity should motivate a change in enzyme description (EC 3.3.2.9) to include additional small strained ring systems, i.e., oxetanes.

In conclusion, we describe the enzyme-catalyzed hydrolysis of a series of simple oxetanes~~yl moieties~~ by mEH. ~~A range of compounds, only differing structurally in the vicinity of the oxetane were hydrolyzed by mEH.~~ The structural requirements for these oxetanyl-containing compounds

DMD Fast Forward. Published on June 9, 2017 as DOI: 10.1124/dmd.117.076489
This article has not been copyedited and formatted. The final version may differ from this version.

to be accepted as substrates and hydrolyzed by mEH efficiently were characterized and the contributions from other enzymes evaluated. These findings will be of value to medicinal chemists designing new oxetane-containing drug candidates. For example, it is not unusual that the metabolic clearance of an investigational drug is highly dependent on e.g. CYP3A4, increasing the risk of drug-drug interactions with co-medications. Introducing an oxetane into a chemistry series may be used as a tool to direct metabolism towards mEH and decreasing the dependence on P450 metabolism. The degree to which this clearance route is tuned in or out can be adjusted using the structural modifications described herein.

This work describes the first stable, non-reactive class of substrates for human mEH, which will allow the reliable measurement of mEH enzyme activity in humans and the scaling from pre-clinical animal species to man. Finally, one can also envision exploitation of mEH as a biocatalyst for racemic oxetane resolution, in a similar manner to the use of e.g. microbial and fungal EHs with epoxides (Hechtberger et al., 1993; Steinreiber and Faber, 2001; Widersten et al., 2010). The structure-metabolism relationship between strained ring-containing drug candidates and mEH is being further explored in ongoing studies on compounds with diverse scaffolds.

Acknowledgements

The Authors thank Drs Bruce Hammock and Christophe Morisseau (UC Davis) for the generous gift of the recombinant enzyme, Dr Sten Nilsson-Lill (AstraZeneca) for helpful discussions on computational methods and Drs Neal Castagnoli Jr. (Virginia Tech) and Erick Carreira (ETH) for the helpful discussions and critical reading of the manuscript.

Authorship contributions

Participated in research design: Toselli, Li, Johansson, Weidolf, Hayes

Conducted experiments: Toselli, Fredenwall

Contributed new reagents or analytic tools: Svensson

Performed data analysis: Toselli, Fredenwall, Svensson, Li, Johansson, Weidolf, Hayes

Wrote or contributed to the writing of the manuscript: Toselli, Fredenwall, Svensson, Li, Johansson, Weidolf, Hayes

References

Armstrong RN (1999) Kinetic and chemical mechanism of epoxide hydrolase. *Drug Metab Rev* **31:**71-86.

Boström J, Hogner A, Llinàs A, Wellner E and Plowright AT (2012) Oxadiazoles in Medicinal Chemistry. *J Med Chem* **55:**1817-1830.

Bull JA, Croft RA, Davis OA, Doran R and Morgan KF (2016) Oxetanes: recent advances in synthesis, reactivity, and medicinal chemistry. *Chem Rev* **116:**12150.

Chacos N, Capdevila J, Falck JR, Manna S, Martin-Wixtrom C, Gill SS, Hammock BD and Estabrook RW (1983) The reaction of arachidonic acid epoxides (epoxyeicosatrienoic acids) with a cytosolic epoxide hydrolase. *Arch Biochem Biophys* **223:**639-648.

de Waziers I, Cugnenc PH, Yang CS, Leroux JP and Beaune PH (1990) Cytochrome P450 isoenzymes, epoxide hydrolase and glutathione transferases in rat and human hepatic and extrahepatic tissues. *J Pharmacol Exp Ther* **253:**387-394.

Emoto C, Murase S, Sawada Y, Jones BC and Iwasaki K (2003) *In vitro* inhibitory effect of 1-aminobenzotriazole on drug oxidations catalyzed by human cytochrome P450 enzymes: a comparison with SKF-525A and ketoconazole. *Drug Metab Pharmacokinet* **18:**287-295.

Eugster HP, Sengstag C, Hinnen A, Meyer UA and Wurgler FE (1991) Heterologous expression of human microsomal epoxide hydrolase in *Saccharomyces cerevisiae*. Study of the valpromide-carbamazepine epoxide interaction. *Biochem Pharmacol* **42:**1367-1372.

Gill SS, Ota K and Hammock BD (1983a) Radiometric assays for mammalian epoxide hydrolases and glutathione S-transferase. *Anal Biochem* **131:**273-282.

Gill SS, Ota K, Ruebner B and Hammock BD (1983b) Microsomal and cytosolic epoxide hydrolases in rhesus monkey liver, and in normal and neoplastic human liver. *Life Sci* **32:**2693-2700.

Gill SS, Wie SI, Guenthner TM, Oesch F and Hammock BD (1982) Rapid and sensitive enzyme-linked immunosorbent assay for the microsomal epoxide hydrolase. *Carcinogenesis* **3:**1307-1310.

Hechtberger P, Wirnsberger G, Mischitz M, Klempier N and Faber K (1993) Asymmetric hydrolysis of epoxides using an immobilized enzyme preparation from *Rhodococcus* sp. *Tetrahedron: Asymmetry* **4:**1161-1164.

Hosagrahara VP, Rettie AE, Hassett C and Omiecinski CJ (2004) Functional analysis of human microsomal epoxide hydrolase genetic variants. *Chem-Biol Interact* **150:**149-159.

Johansson A, Lofberg C, Antonsson M, von Unge S, Hayes MA, Judkins R, Ploj K, Benthem L, Linden D, Brodin P, Wennerberg M, Fredenwall M, Li L, Persson J, Bergman R, Pettersen A, Gennemark P and Hogner A (2016) Discovery of (3-(4-(2-Oxa-6-azaspiro[3.3]heptan-6-ylmethyl)phenoxy)azetidin-1-yl)(5-(4-methoxy phenyl)-1,3,4-oxadiazol-2-yl)methanone (AZD1979), a Melanin Concentrating Hormone receptor 1 (MCHr1) antagonist with favorable physicochemical properties. *J Med Chem* **59:**2497-2511.

Kerr BM, Rettie AE, Eddy AC, Loiseau P, Guyot M, Wilensky AJ and Levy RH (1989) Inhibition of human liver microsomal epoxide hydrolase by valproate and valpromide: *in vitro/in vivo* correlation. *Clin Pharm Ther* **46:**82-93.

Kitteringham NR, Davis C, Howard N, Pirmohamed M and Park BK (1996) Interindividual and interspecies variation in hepatic microsomal epoxide hydrolase activity: studies with *cis*-stilbene oxide, carbamazepine 10, 11-epoxide and naphthalene. *J Pharmacol Exp Ther* **278:**1018-1027.

Kroetz DL, Loiseau P, Guyot M and Levy RH (1993) *In vivo* and *in vitro* correlation of microsomal epoxide hydrolase inhibition by progabide. *Clin Pharm Ther* **54:**485-497.

Li XQ, Hayes MA, Gronberg G, Berggren K, Castagnoli N, Jr. and Weidolf L (2016) Discovery of a novel microsomal epoxide hydrolase-catalyzed hydration of a spiro oxetane. *Drug Metab Dispos* **44:**1341-1348.

Liu JY, Park SH, Morisseau C, Hwang SH, Hammock BD and Weiss RH (2009) Sorafenib has soluble epoxide hydrolase inhibitory activity, which contributes to its effect profile *in vivo*. *Mol Cancer Ther* **8:**2193-2203.

Morisseau C, Bernay M, Escaich A, Sanborn JR, Lango J and Hammock BD (2011) Development of fluorescent substrates for microsomal epoxide hydrolase and application to inhibition studies. *Anal Biochem* **414:**154-162.

Morisseau C and Hammock BD (2005) Epoxide hydrolases: mechanisms, inhibitor designs, and biological roles. *Annu Rev Pharmacol Toxicol* **45:**311-333.

Morisseau C and Hammock BD (2007) Measurement of soluble epoxide hydrolase (sEH) activity. *Curr Protoc Toxicol* **Chapter 4:**Unit 4 23.

Muller F, Arand M, Frank H, Seidel A, Hinz W, Winkler L, Hanel K, Blee E, Beetham JK, Hammock BD and Oesch F (1997) Visualization of a covalent intermediate between microsomal epoxide hydrolase, but not cholesterol epoxide hydrolase, and their substrates. *Eur J Biochem* **245:**490-496.

Oesch F, Herrero ME, Hengstler JG, Lohmann M and Arand M (2000) Metabolic detoxification: implications for thresholds. *Toxicol Pathol* **28:**382-387.

Pacifici GM, Franchi M, Bencini C and Rane A (1986) Valpromide inhibits human epoxide hydrolase. *Br J Clin Pharmacol* **22:**269-274.

Rioux N, Duncan KW, Lantz RJ, Miao X, Chan-Penebre E, Moyer MP, Munchhof MJ, Copeland RA, Chesworth R and Waters NJ (2016) Species differences in metabolism of

EPZ015666, an oxetane-containing protein arginine methyltransferase-5 (PRMT5) inhibitor. *Xenobiotica* **46:**268-277.

Seidegard J and DePierre JW (1980) Benzil, a potent activator of microsomal epoxide hydrolase *in vitro*. *Eur J Biochem* **112:**643-648.

Song W, Yu L and Peng Z (2015) Targeted label-free approach for quantification of epoxide hydrolase and glutathione transferases in microsomes. *Anal Biochem* **478:**8-13.

Steinreiber A and Faber K (2001) Microbial epoxide hydrolases for preparative biotransformations. *Curr Opin Biotechnol* **12:**552-558.

Stepan AF, Karki K, McDonald WS, Dorff PH, Dutra JK, DiRico KJ, Won A, Subramanyam C, Efremov IV, O'Donnell CJ, Nolan CE, Becker SL, Pustilnik LR, Sneed B, Sun H, Lu YS, Robshaw AE, Riddell D, O'Sullivan TJ, Sibley E, Capetta S, Atchison K, Hallgren AJ, Miller E, Wood A and Obach RS (2011) Metabolism-directed design of oxetane-containing arylsulfonamide derivatives as gamma-secretase inhibitors. *J Med Chem* **54:**7772-7783.

Thomas PE, Ryan DE, von Bahr C, Glaumann H and Levin W (1982) Human liver microsomal epoxide hydrolase. Correlation of immunochemical quantitation with catalytic activity. *Mol Pharmacol* **22:**190-195.

Tzeng H-F, Laughlin LT, Lin S and Armstrong RN (1996) The catalytic mechanism of microsomal epoxide hydrolase involves reversible formation and rate-limiting hydrolysis of the alkyl-enzyme intermediate. *J Am Chem Soc* **118:**9436-9437.

Vaclavikova R, Hughes DJ and Soucek P (2015) Microsomal epoxide hydrolase 1 (EPHX1): gene, structure, function, and role in human disease. *Gene* **571:**1-8.

Widersten M, Gurell A and Lindberg D (2010) Structure-function relationships of epoxide hydrolases and their potential use in biocatalysis. *Biochim Biophys Acta* **1800:**316-326.

Wuitschik G, Carreira EM, Wagner B, Fischer H, Parrilla I, Schuler F, Rogers-Evans M and Muller K (2010) Oxetanes in drug discovery: structural and synthetic insights. *J Med Chem* **53:**3227-3246.

Footnotes

This work was presented in preliminary form at the 21st International Symposium on Microsomes and Drug Oxidations in Davis, California, 2-6, October 2016, USA.

Reprint requests should be addressed to Dr M. A. Hayes, Cardiovascular and Metabolic Diseases, Innovative Medicines and Early Development, AstraZeneca, Pepparedsleden 1, Mölndal, 431 83, Sweden. E: martin.hayes@astrazeneca.com

DMD Fast Forward. Published on June 9, 2017 as DOI: 10.1124/dmd.117.076489
This article has not been copyedited and formatted. The final version may differ from this version.

Figure legends

Figure 1

Metabolism of compound 5.

UHPLC-MS extracted ion chromatograms are shown for: (A) **5** and its metabolites formed after a 60-min incubation with HLM and NADPH; (B) synthetic diol **11**. Peak labels are *m/z* values and correspond to: parent (*m/z* 465.21); hydrolysis (*m/z* 483.22); oxidation (*m/z* 481.21); demethylation (*m/z* 451.20); hydrolysis plus demethylation (*m/z* 469.21).

Figure 2

Tentative fragmentation pattern (A) and MS^E spectra of compound 5 (B), of its diol metabolite formed in incubations with HLM (C) and of the synthesized diol 11 (D). Insets are full-scan MS spectra.

Figure 3

Effect of P450 inhibitors ketoconazole (KTZ) and 1-aminobenzotriazole (1-ABT), the mEH inhibitor valpromide (VPD) and the sEH inhibitor *t*-AUCB (20 µM) on the hydration of compound 6.~~**Inhibition of hydrolysis of 6 by the P450 inhibitor ketoconazole (KTZ) and the mEH inhibitor valpromide (VPD), after a 60-min incubation with HLM**~~**.**

HLM, human liver microsomes; hHeps, human hepatocytes; HLC, human liver cytosol. Assay conditions were: 10 µM substrate, 60-min incubation with 1 mg/ml HLM or HLC protein; and 4 µM substrate, 2-hour incubation with 10^6 hepatocytes/ml. Results are expressed as a % of the diol formed in reactions with NADPH and no inhibitor (CTRL), and bars are averages of duplicate measurements + range. Similar results were also obtained with the mEH inhibitor progabide.

DMD Fast Forward. Published on June 9, 2017 as DOI: 10.1124/dmd.117.076489
This article has not been copyedited and formatted. The final version may differ from this version.

Table 1. Physico-chemical properties of compounds **1-9** and percentage of dihydrodiol metabolites formed in incubations with ~~compounds **1-9** and~~ human liver microsomes.

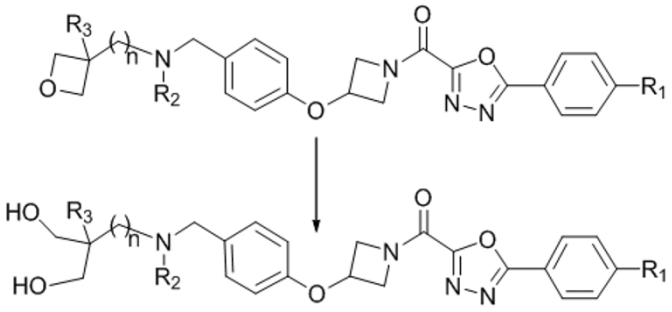

#	R^1	R^2	R^3	n	Solubility[a] (µM)	LogD[a]	pK_a[a]	Average % dDiol in HLM (replicate 1, replicate 2)[b]
1	MeO	Me	H	0	11	3.0	6.1	0 (0, 0)
2	H	H	H	0	106	2.1	6.6	1.1 ~~± 0.1~~(1.2, 0.9)
3	MeO	H	H	0	63	2.2	6.6	1.6 ~~± 0.1~~(1.6, 1.7)
4	H	H	Me	1	858	2.3	8.4	15 ~~± 0~~(15, 15)
5	MeO	H	Me	1	NA	2.0	8.2	16 ~~± 0~~(16, 16)
6	H	Me	Me	1	80	4	8.5	91 ~~± 1~~(89, 92)
7	MeO	Me	Me	1	70	4.1	8.0	89 ~~± 0~~(88, 89)
8	MeO	H	H	1	NA	1.3	NA	2.7 ~~± 0~~(2.7, 2.8)
9	MeO	H	Me	0	NA	2.3	6.9	< 1

[a] Solubility, $logD_{7.4}$ HPLC and pK_a ~~was~~ were measured as described earlier (Boström et al., 2012); NA, not available. [b] HLM, human liver microsomes. ~~Average d~~Diol levels ~~± range~~ were determined from duplicate incubations (60 min) of 10 µM substrate with HLM, without NADPH. Diol metabolite levels are expressed as a percentage of the sum of parent + diol peak areas.

Table 2. Physico-chemical properties of compounds **15-20** and percentage of dihydrodiol metabolites formed in incubations with human liver microsomes.

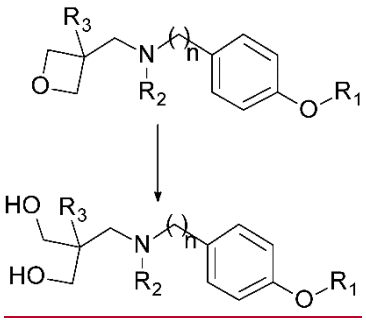

#	R^1	R^2	R^3	n	Solubility[a] (µM)	LogD[a]	pK_a[b]	Average % diol in HLM, (replicate 1, replicate 2)[c]
15	Me	Me	Me	1	258	1.6	8.2	9.9 (10.0, 9.9)
16	Me	Me	Me	1	586	0.4	9.3	1.5 (0, 3.1)
17	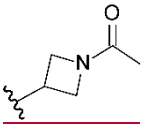	Me	Me	1	950	0.8	8.2	2.3 (2.1, 2.5)
18	Me	Me	Me	2	612	1.6	8.9	3.1 (3.0, 3.1)
19	Me	H	Me	2	628	0.5	9.7	0.7 (0.7, 0.7)
20	Me	Me	H	2	587	1.0	8.9	0 (0, 0)

[a]Solubility and $logD_{7.4}$ HPLC were measured as decribed earlier (Boström et al., 2012); [b]calculated values; [c]HLM, human liver microsomes; diol levels were determined from duplicate incubations (60 min) of 10 µM substrate with HLM, without NADPH. Diol metabolite levels are expressed as a percentage of the sum of parent + diol peak areas.

DMD Fast Forward. Published on June 9, 2017 as DOI: 10.1124/dmd.117.076489
This article has not been copyedited and formatted. The final version may differ from this version.

Table ~~2~~3. Kinetic parameters for dihydrodiol formation in reactions with compounds **4-7, 15** and **18**[a].

	Human recombinant mEH[b]			HLM without NADPH[c]		
#	K_m (µM)	V_{max} (nmol/min/mg)	V_{max}/K_m	K_m (µM)	V_{max} (nmol/min/mg)	V_{max}/K_m
4	67±10	17±1	0.26	27±5	1.7±0.1	0.06
5	47 (43, 59)~~±5~~	17~~±1~~ (17, 17)	0.36	26±6	1.7±0.1	0.07
6	89±14	22±2	0.24	28±8	6.6±0.7	0.27
7	50±7	35±2	0.69	51 (48, 56)~~±16~~	1~~65~~ (15, 16)~~±2~~	0.31~~29~~
15		[b]		352 (239, 695)	0.9 (0.8, 1.4)	0.003
18	684 (650, 722)	2.8 (2.7, 3.0)	0.004	139 (119, 165)	0.4 (0.3, 0.4)	0.003
***c*SO**[~~d~~c]	141	570	4	7-25	17-52	2.1-2.5
SO[~~d~~e]	-	-	-	40-300	10-25	0.05-0.4

[a] Values are mean of triplicates ± standard error, except for compound **5, 15** and **18** incubated with recombinant mEH and compound **7, 15** and **18** incubated with HLM, for which duplicates average (replicate 1, replicate 2) are reported. mEH, microsomal epoxide hydrolase; HLM, human liver microsomes. Product formation was linear with respect to time and enzyme concentration. [b] Kinetic parameters could not be estimated as the velocity remained linear within

the substrate concentration range chosen. ~~Incubations with recombinant mEH: n=2 for compound 5, and n=3 for all other compounds.~~ [e] ~~Incubations with HLM: n=2 for compound 7, and n=3 for all other compounds.~~ [dc] Values from (Kitteringham et al., 1996; Hosagrahara et al., 2004; Morisseau et al., 2011). [de] SO, styrene oxide; ~~V~~values from (Seidegard and DePierre, 1980; Pacifici et al., 1986; Eugster et al., 1991).

DMD Fast Forward. Published on June 9, 2017 as DOI: 10.1124/dmd.117.076489
This article has not been copyedited and formatted. The final version may differ from this version.

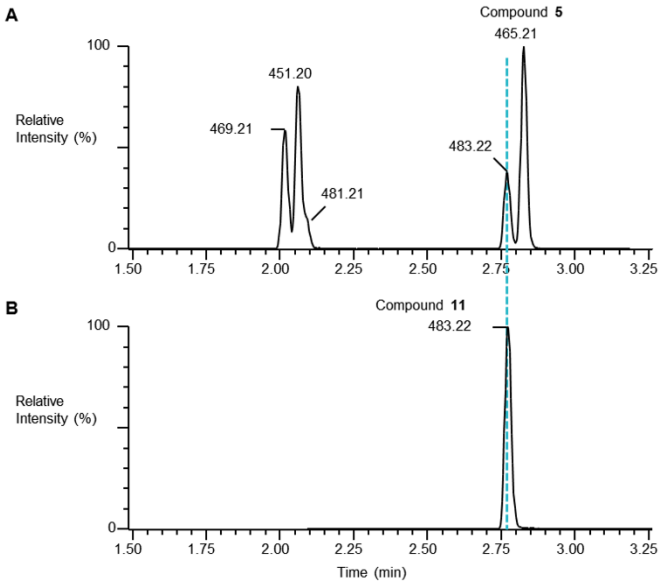

Figure 1.

DMD Fast Forward. Published on June 9, 2017 as DOI: 10.1124/dmd.117.076489
This article has not been copyedited and formatted. The final version may differ from this version.

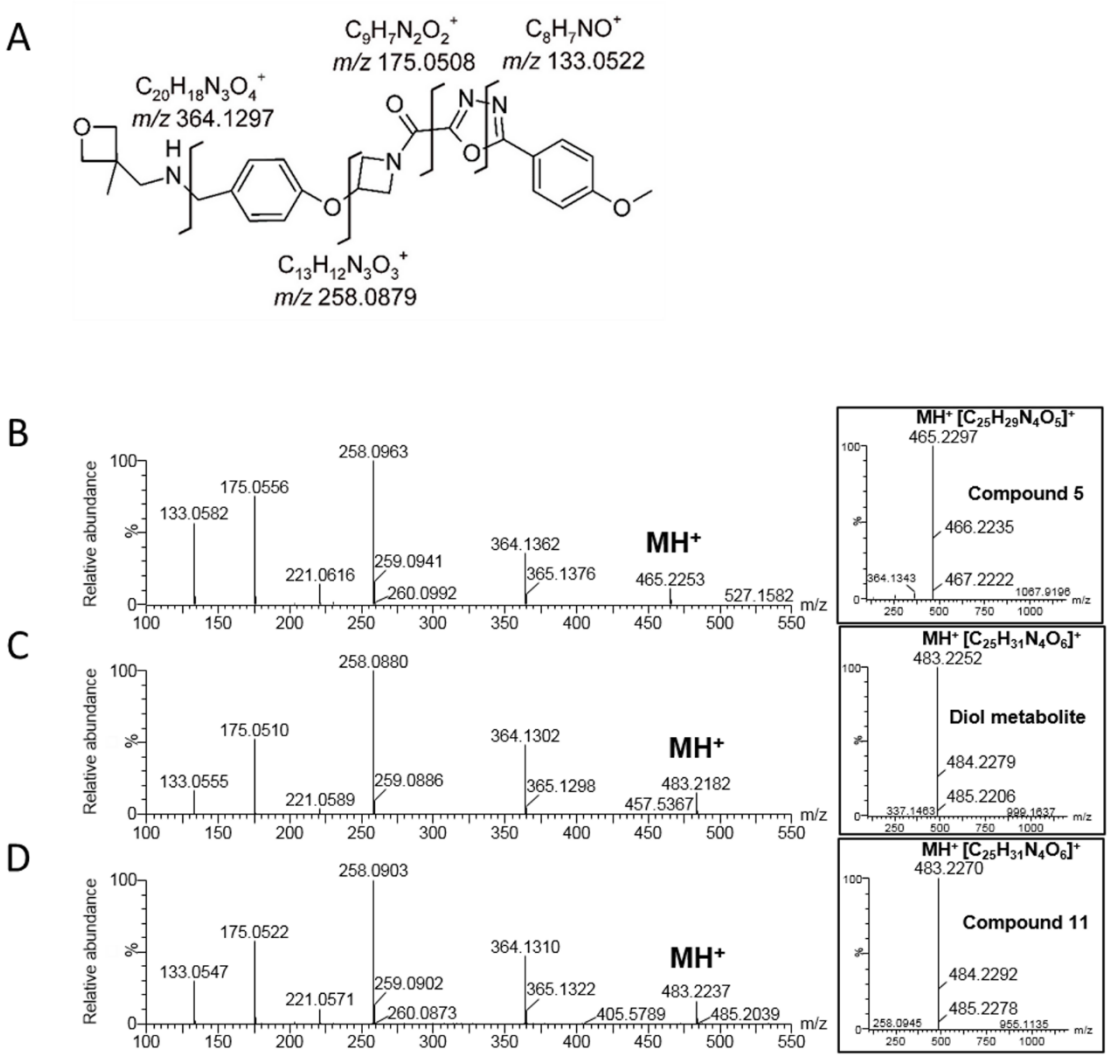

Figure 2.

DMD Fast Forward. Published on June 9, 2017 as DOI: 10.1124/dmd.117.076489
This article has not been copyedited and formatted. The final version may differ from this version.

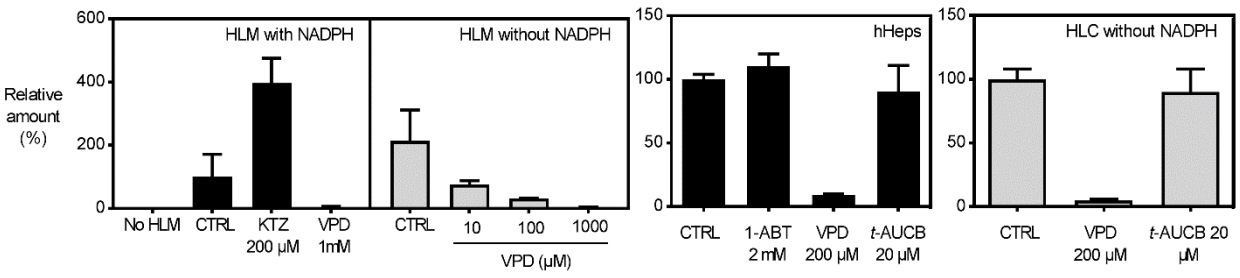

Figure 3.